BIOCHEMISTRY
including biophysical chemistry & molecular biology

Article

pubs.acs.org/biochemistry

Mass Spectrometry-Based Protein Footprinting Characterizes the Structures of Oligomeric Apolipoprotein E2, E3, and E4

Brian Gau,[†] Kanchan Garai,[‡] Carl Frieden,[‡] and Michael L. Gross*[,†]

[†]Department of Chemistry, Washington University, One Brookings Drive, St. Louis, Missouri 63130, United States

[‡]Department of Biochemistry and Molecular Biophysics, Washington University School of Medicine, 660 South Euclid, St. Louis, Missouri 63110, United States

Supporting Information

ABSTRACT: The three common isoforms of apolipoprotein E (ApoE) differ at two sites in their 299 amino acid sequence; these differences modulate the structure of ApoE to affect profoundly the isoform associations with disease. The ε4 allele in particular is strongly associated with Alzheimer's disease. The study of the structural effects of these mutation sites in aqueous media is hampered by the aggregation proclivity of each ApoE isoform. Hence, understanding the differences between isoforms has thus far relied on lower resolution biophysical measurements, mutagenesis, homology studies, and the use of truncated ApoE variants. In this study, we report two comparative studies of the ApoE family by using the mass spectrometry-based protein footprinting methods of FPOP and glycine ethyl ester (GEE) labeling. The first experiment examines the three full-length WT isoforms in their tetrameric state and finds that the overall structures are similar, with the exception of M108 in ApoE4 which is more solvent-accessible in this isoform than in ApoE2 and ApoE3. The second experiment provides clear evidence, from a comparison of the footprinting results of the wild-type proteins and a monomeric mutant, that several residues in regions 183−205 and 232−251 are involved in self-association.

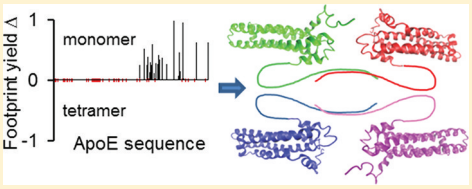

Apolipoprotein E is a 34 kDa protein whose function is to regulate lipid metabolism and control lipid redistribution in tissue and cells, especially in the brain.[1] The three most common isoforms differ at two residues; apolipoprotein E2 (ApoE2) has cysteines at sites 112 and 158, whereas apolipoprotein E4 (ApoE4) has arginines at these residue sites. The most common isoform, apolipoprotein E3 (ApoE3), has C112 and R158. The ApoE4 isoform is strongly associated with Alzheimer's disease[2,3] and is a risk factor for several other diseases.[4] These risk associations, which ultimately stem from the single substitution C112R, differentiate ApoE4 from ApoE2 and ApoE3 in the preferred lipoprotein particle structure.[5] Structural determinations by X-ray crystallography and solution NMR of the lipid-free N-terminal domain showed it to be an elongated four-helix bundle.[6,7] Since then, no high-resolution structures have been reported for the wild-type isoforms or their C-terminal domains in the lipid-free state owing to their propensity to oligomerize.

The three ApoE isoforms each self-associate in a lipid-free solution, forming predominantly tetramers at micromolar concentration.[8−12] The rate constants for the monomer−dimer−tetramer association−dissociation process were determined by Garai and Frieden.[8] On the basis of the most recent high-resolution structure determination of the N-terminal domain, Sivashanmugam and Wang[7] proposed a scheme whereby lipid binding opens the N-terminal four-helix bundle, allowing further lipid interaction. Potentially affecting this or other mechanisms of lipid interaction in an isoform-specific manner are the lipid-free domain interaction and kinetics of oligomerization. To inform these inferences, we undertook an implicit analysis of the full-length WT isoform structures at "residue resolution" by using mass spectrometry (MS)-based protein footprinting. The overarching question we pose is whether the amino acid accessibilities of full-length ApoE2, ApoE3, and ApoE4 isoforms differ in their oligomeric states at micromolar concentrations. We also seek to identify those regions responsible for oligomeric interactions by comparing the protein footprints of WT ApoE3 with those of a monomeric mutant of ApoE3. Recently an NMR structure of this monomeric mutant has been determined.[13]

MS-based protein footprinting provides peptide and residue-resolved structural information in the primary sequence dimension.[14,15] The general strategy provides insight about the difference between the structure of a protein or a protein assembly in two or more states rather than resolving their structures in three dimensions. The expectation is that labeling at solvent-accessible residues is attenuated at protein−ligand or protein−protein interfaces in the complex compared to those residues in the apo state. The approach is effective and efficient because, if the labeling is stable, identification of the modification sites can be done by using a proteomics-based, "bottom-up" mass spectrometry methodology.[16] In this methodology, proteolytic peptides are chromatographically resolved and detected in a hybrid mass spectrometer capable of monitoring their accurate mass-to-charge ratios at high mass

Received: June 14, 2011
Revised: July 27, 2011
Published: August 17, 2011

resolving power. The second spectrometer in the hybrid acquires the characteristic product-ion spectra of peptide ions subjected to collisional activation in an elution-dependent manner. The high-resolution LC-MS intensities provide a semiquantitative measure of each peptide, and their product ion spectra, acquired in this tandem MS mode (MS^2), can indicate their identity and modification site(s).

An informative chemical footprinting method is hydroxyl radical-mediated modification of solvent accessible side chains. (For a comprehensive review detailing several methodologies for •OH generation, expected product chemistry, and MS analysis, see ref 17.) Hydroxyl radical labeling is advantageous because it probes solvent accessibility, given that •OH has the same size as water, and it imparts stable covalent modifications to solvent-accessible side chains of over half of the common amino acids.[18] Here we used the method of fast photochemical oxidation of proteins (FPOP), a method developed by Hambly and Gross that is similar to but has some important differences with that of Aye and co-workers.[19,20] In the FPOP method, low millimolar levels of H_2O_2 are homolytically cleaved by a 17 ns flash of 248 nm light from a KrF excimer laser source. The resultant •OH reacts with the side chains of constituent proteins. An important feature of FPOP is that the reaction time scale can be controlled; in the presence of the scavenger glutamine, the lifetime of the •OH is ~1 μs. The use of a radical scavenger ensures that only equilibrium conformations are sampled by •OH; any modification-induced changes to conformation evolve on a longer time scale and are not sampled by the labeling.[19,21] To corroborate the FPOP results, we also employed a method of acidic-side-chain footprinting, using glycine ethyl ester (GEE) and a zero-length cross-linker.[22−24]

EXPERIMENTAL PROCEDURES

Reagents. Acetonitrile, acetic acid, formic acid, 30% hydrogen peroxide, L-glutamine, L-methionine, tris(2-carboxyethyl)phosphine hydrochloride (TCEP), catalase, guanidinium hydrochloride, glycine ethyl ester (GEE), 1-ethyl-3-(3-(dimethylamino)propyl)-carbodiimide (EDC), 2-amino-2-hydroxymethylpropane-1,3-diol (Tris base), and phosphate buffered saline (PBS) were purchased from Sigma-Aldrich Chemical Co. (St. Louis, MO). Sequencing grade trypsin was purchased from Roche Diagnostics Corp. (Indianapolis, IN). Purified water (18 MΩ) was obtained from a Milli-Q Synthesis system (Millipore, Billerica, MA).

Protein Expression, Mutagenesis, Purification, and Solubilization. ApoE2, ApoE3, ApoE4, and the monomeric mutant of ApoE3 (ApoE3MM) were expressed in *E. coli* as described elsewhere.[25] The proteins were dissolved in 6 M guanidinium chloride and dialyzed overnight into phosphate buffered saline (PBS) solution containing 100 μM TCEP disulfide reductant. Protein concentrations were determined by measuring their 280 nm absorbance using ε_{280} = 44 950 M^{-1} cm^{-1}. The resultant solutions were stored as aliquots at −80 °C after $N_2(l)$ freezing.

FPOP Labeling. The FPOP labeling of ApoE3MM and ApoE3 in the monomer/oligomer experiment was performed on the same day under the same conditions for both proteins. Each started with a 3 h, 22 °C equilibration of 4 μM protein containing 20 mM Gln and 100 μM TCEP in PBS. Three replicates were drawn from each of these solutions for FPOP labeling. Just prior to FPOP, H_2O_2 was added to each replicate by 10-fold dilution from a concentrated solution, to give a final concentration of 40 mM. The FPOP apparatus was essentially the same as originally described.[19] The KrF excimer laser power (GAM Laser Inc., Orlando, FL) was adjusted to 39 mJ/pulse and its pulse frequency set to 5 Hz. The flow rate was adjusted to ensure a 25% exclusion volume to avoid repeat •OH exposure.[21] Each replicate was collected in a microcentrifuge tube containing 10 μL of 200 fM catalase and Met to give a final concentration of 20 mM in the total sample volume. The addition of Met mitigates post-FPOP oxidation of protein.[26] Catalase was allowed to oxidize H_2O_2 to $O_2(g)$ for 10 min at room temperature with pipet mixing; $O_2(g)$ was removed by three centrifugation steps during the incubation. After 10 min, samples were frozen by immersion in $N_2(l)$ and stored at −80 °C prior to proteolysis. Control samples were handled in the same manner as those submitted to FPOP, but they were not laser irradiated; instead, they were incubated for 5 min with H_2O_2, after which the solution was added to the catalase−methionine collection volume. The FPOP labeling of WT-ApoE2, ApoE3, and ApoE4 was performed as described above with the following exceptions: the final H_2O_2 concentration was 20 mM, and the excimer laser power was measured to be 47 mJ/pulse.

Carboxylic Acid Labeling with GEE. For the monomer/oligomer experiment, samples were drawn from the same ApoE3 and ApoE3MM equilibrated solution as was used for FPOP labeling, at approximately the same time. GEE was added to a final concentration of 50 mM to each equilibrated solution. Samples were drawn from this solution, and EDC was added to each to give a final concentration of 5 mM. One molar acetic acid was added to a final concentration of 0.5 M to quench the reaction after a certain incubation period starting with the addition of EDC. Time-dependent data were obtained for GEE/EDC exposures times of 1, 3, 6, and 12 min for labeled ApoE3 and ApoE3MM samples, in duplicate, to provide a data trend. Samples were frozen in $N_2(l)$ and stored at −80 °C prior to proteolysis.

Proteolysis. GEE-labeled samples were thawed and purified with Millipore $Ziptip_{C4}$ prior to proteolysis; the 50% acetonitrile eluent was diluted 10-fold with 250 mM Tris buffer, pH 7.3. FPOP-labeled and control samples were thawed and used as such for proteolysis. All samples were proteolyzed with 8:1 protein:trypsin (by weight) at 37 °C for 3 h. ESI MS of several control replicates on a Bruker Maxis Q-TOF verified that the digestion was complete. The samples were concentrated 3-fold by SpeedVac drying at 30 °C and then desalted by Millipore $Ziptip_{C18}$, with elution into 10 μL of 50% acetonitrile 1% formic acid solution. A portion of this was diluted 25-fold with water and 0.1% formic acid for autosampler loading and subsequent analysis.

LC-MS/MS Acquisition. The experiments were not analyzed by LC-MS/MS contiguously; a new column was packed for each, and the nanospray source conditions varied slightly for each analysis. Five microliters of each replicate was loaded by autosampler onto a 20 cm column with a PicoFrit tip (New Objective, Inc., Woburn, MA), bomb-packed with C18 reverse phase material (Magic, 0.075 mm × 200 mm, 5 μm, 300 Å, Michrom, Auburn, CA). Peptides were eluted by a 70 min, 260 nL/min gradient coupled to the nanospray source of an LTQ-Orbitrap mass spectrometer (Thermo Fisher, Waltham, MA). Mass spectra were obtained at high mass resolving power (100 000 for ions of m/z 400) on the Orbitrap component, and the six most abundant ions eluting per scan were each subjected to CID MS^2 experiment in the LTQ component, using a collision energy 35% of the maximum, a 2 Da isolation width,

and wideband activation. Precursor ions were added to a dynamic exclusion list for 8 s to ensure good sampling of the apex of their elution peaks. A blank was run between every sample acquisition.

Data Analysis. The Rosetta Elucidator data management system (Rosetta Biosoftware) was used to generate tables of all LC-MS features eluting in time at high m/z resolution (±5 ppm); all quantitation was based on ion abundances from extracted ion chromatograms. Usually more than one high-resolution feature mapped to a single eluting peptide, owing to the splitting of its ion signal among multiple charge states and isotopomers. All such features contributed to the measure of total peptide abundance. Most modified and unmodified peptide features were annotated by error-tolerant Mascot database searching (Matrix Science, Boston, MA), with the common •OH outcomes added to its variable modification database.[17] An Excel visual basic-assisted strategy was employed to validate questionable Mascot-error tolerant calls. Ultimately the CID product-ion spectra of over two-thirds of all calls were checked manually. Additional features having no Mascot annotations were included if their ions' m/z matched those of putative tryptic ApoE-modified or unmodified peptides within 8 ppm, and they had product-ion spectra that were consistent (manual interpretation) with these calls. This manual validation was assisted by using a custom correlation algorithm that compared these spectra to exemplary CID fragment spectra of unmodified tryptic peptides of the WT isoforms and ApoE3MM.[27]

The labeling yield per residue is determined according to eq 1.

$$\begin{aligned} &i\text{th residue yield} \\ &=\Big(\sum \text{peptide abundances modified at residue } i\Big) \\ &\quad /\Big(\sum \text{peptide abundances with same} \\ &\quad \text{sequence as numerator peptides}\Big) \end{aligned} \tag{1}$$

Equation 1 avoids a potential underestimation bias by excluding the measured abundances for peptides in the denominator, whose modified siblings did not give CID MS^2 spectra definitively locating their modification sites (and hence cannot populate the numerator). Typically these peptides contain one or more missed-trypsin-cleavage site(s). With the exception of one modification of Arg, FPOP does not introduce a proteolytic bias that could undermine eq 1 because the frequency of missed cleavages is shared by control and FPOP samples. We do observe a low abundance of the •OH-mediated loss of 43 u as a portion of the guanidino group of Arg;[17] we have not included these low-abundant data because of their clear influence on trypsin proteolysis.

RESULTS

Data Acquisition and Processing. We determined the FPOP footprints of the WT isoforms existing as oligomers, as they do at low micromolar concentrations.[8,10,11,28,29] (Supporting Information Table 1 presents the per-residue FPOP yields determined from all validated LC-MS features.) In this residue-resolved analysis, 206 unmodified and modified tryptic peptides of the isoforms (Supporting Information Table 2) were tracked from 1457 extracted ion LC-MS chromatographic (EIC) ions, comprising 67.8% of all eluting ions. We were able to find peptides from all regions of the protein after FPOP labeling and trypsin proteolysis, except for the region 39-61. Although peptide 39-61 is detectable as unmodified, it was not well sampled upon FPOP owing to its low abundance or response. Nevertheless, approximately one in five residues was FPOP-modified at 0.1% or greater yield.

The results are presented as a difference in labeling yield per residue as normalized to the maximum labeling yield for all residues of the same amino acid type (Figures 1, 2, and 3). A positive value indicates more labeling in the comparison protein (ApoE2 or ApoE4) than at the same site in WT ApoE3. Negative values convey the opposite trend. The extent of labeling is a function of the solvent-accessible surface area (SASA) of a site and its inherent fully solvent-exposed reactivity with •OH. We observe a linear correlation between the SASA of residues of the same amino acid type and their FPOP yield (data not shown). Thus, by normalizing each residue's yield by the maximum FPOP yield among all same-amino acid residues, the inherent reactivity dependence is eliminated, and we may compare the yields of different-amino acid residues. Furthermore, the normalization of the yield difference between isoforms ensures that a departure from near zero labeling at a residue is not misinterpreted as complete exposure of the residue in one protein state and complete concealment in its comparison state.

WT-ApoE2 vs ApoE3 vs ApoE4. The extent of modification per residue for WT-ApoE2, ApoE3, and ApoE4 are very similar, although ApoE4 exhibits more differences with ApoE3 than does ApoE2. In Figure1A, all detected residues shared by ApoE3 and ApoE4 are shown. Only M108, Y162, P183, V185, and E266 are significantly different at a 95% confidence by Student's t test. In Figure 2A, all detected residues shared by ApoE3 and ApoE2 are shown. Tyrosine 162, E255, and E266 are significantly different. If the uncertainties in yield measurements were zero, the differences in labeling, and therefore in solvent accessibility change, are small for the majority of the residues. Comparing ApoE4 to ApoE3, 43 of 56 residues exhibit a change of less than 15% relative to the maximum SASA of each kind of amino acid in the proteins. Comparing ApoE2 to ApoE3, 49 of 56 residues also exhibit a maximum amino acid area relative change of less than 15%.

The extent of modification per peptide between the isoforms is also similar (Figures 1B and 2B). The analysis at the peptide level affords the inclusion of 24 more features than the analysis at the residue level (Supporting Information Table 2). These additional features' modification sites could not be resolved, because either the feature was a complex mixture of modified peptide isomers or the peptides did not detectably fragment in the region of the modification in the MS^2 experiment. Consequently, though each added feature's precursor mass was within 5 ppm of a theoretical ApoE peptide mass, and each had an product-ion (MS^2) spectrum that confirmed the identity of the root peptide sequence, it could not be used in a per-residue yield analysis. To omit these from the per-peptide yield analysis, however, introduces an underestimation bias. Thus, the inclusion of these features provides for the most accurate measure of the peptide FPOP-labeling yield. Comparing ApoE4 to ApoE3 (Figure 1B), 22 of 29 peptides exhibited statistically identical labeling yields. Peptides spanning 62-72, 120-134, and 261-274 each exhibit slightly more labeling in ApoE4 than ApoE3, whereas 104-112 is significantly more labeled in ApoE3. Comparing ApoE2 to ApoE3 (Figure 2B), only peptide 62-68 is significantly different, with less labeling in ApoE2.

The wild-type isoforms are similar in their response to FPOP labeling and the residue-resolved differences are small

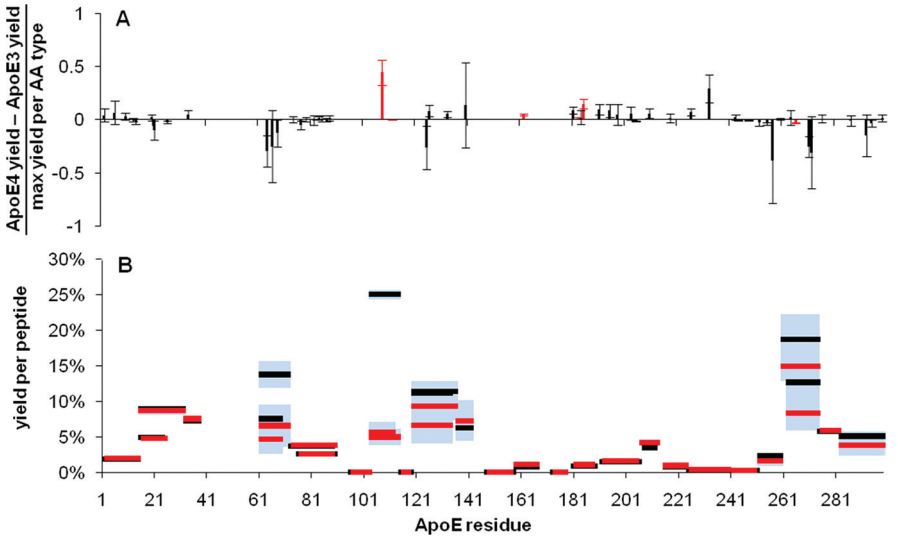

Figure 1. Comparison of the tryptic-peptide-resolved and residue-resolved FPOP labeling yields for ApoE3 and ApoE4. Panel A plots the difference in yield per residue between isoforms, relative to the maximum yield per residue for all residues of the same amino acid type. Background modification yields observed in the control experiments are subtracted from their corresponding FPOP yields before the relative value is determined. Error bars are propagated from the standard errors of the per-residue average labeling yields for ApoE3 FPOP, ApoE3 control, ApoE4 FPOP, and ApoE4 control treatments. Residues M108, Y162, P183, V185, and E266, shown in red in panel A, are significantly different between isoforms at 95% confidence by the Student's *t* test. Panel B plots the FPOP labeling yield/tryptic peptide of ApoE3 in black and ApoE4 in red. The background modification fraction per peptide has been subtracted. The light-blue areas convey the standard error of each labeling measurement. Where peptides exhibit very similar labeling levels, the red ApoE4 bar may obscure the ApoE3 black bar.

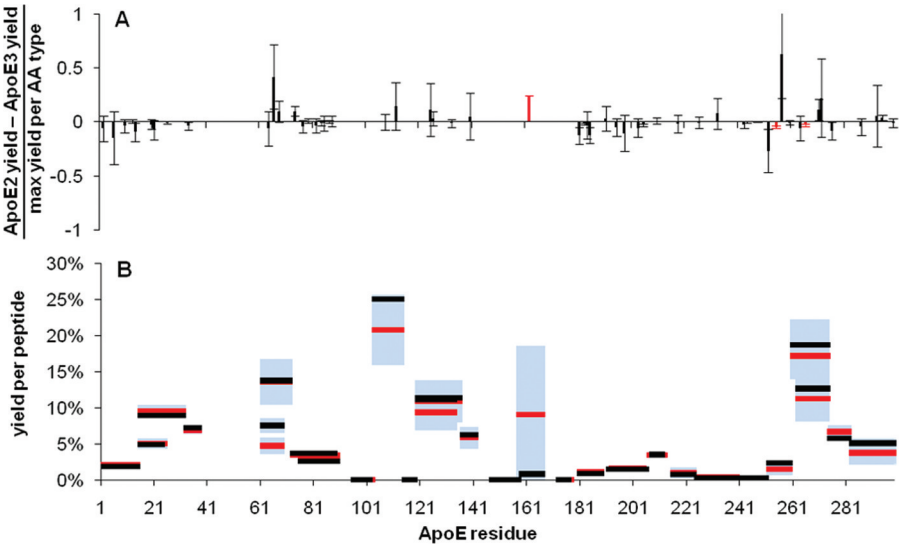

Figure 2. Comparison of the tryptic-peptide-resolved and residue-resolved FPOP labeling yields for ApoE2 and ApoE3. Panel A plots the difference in yield per residue between isoforms, relative to the maximum yield per residue for all residues of the same amino-acid type. Background modification yields observed in the control experiments are subtracted from their corresponding FPOP yields before the relative value is determined. Error bars are determined as described in Figure 1. Residues Y162, E255, and E266, shown in red in panel A, are significantly different between isoforms at 95% confidence by the Student's *t* test. Panel B plots the FPOP labeling yield/tryptic peptide of ApoE3 in black and ApoE2 in red. The background modification fraction per peptide has been subtracted. The light-blue areas convey the standard error of each labeling measurement. Where peptides exhibit very similar labeling levels, the red ApoE2 bar may obscure the ApoE3 bar.

compared to the maximum level of labeling measured per amino acid type. The one exception to this trend is M108. Its modification level is 5 ± 1% for ApoE4, whereas M108 undergoes negligible modification for ApoE2 and ApoE3. This effect was missed with peptide-level analysis because a major source of modification signals in ApoE3 104-114 is at C112, owing to the high •OH reactivity of cysteine; ApoE4 104-112 and ApoE4 104-114 tryptic peptides lack this labeling-sensitive site. The residue-level difference at M108 suggests a structural difference in the region of ApoE4 with respect to the other isoforms. It is also possible that C112 suppresses nearby M108 •OH-mediated labeling in ApoE3.[30]

The modification extent for 158-167 of ApoE2 (Figure 2B) is also high because its primary modification is of C158; ApoE3

dx.doi.org/10.1021/bi200911c | *Biochemistry* 2011, 50, 8117–8126

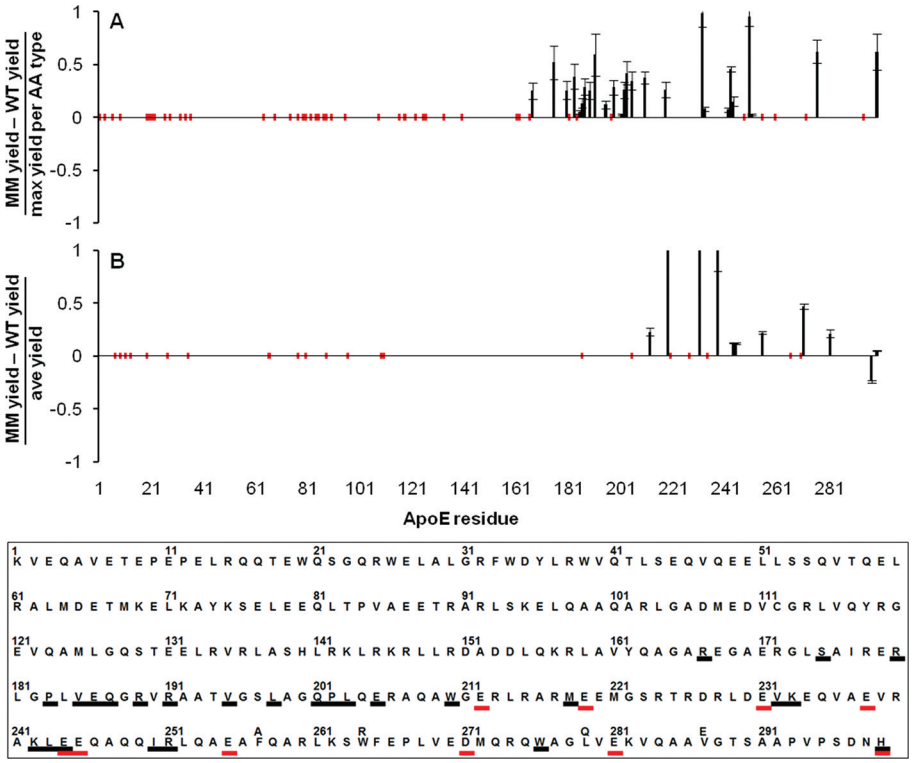

Figure 3. Comparison of the tryptic-peptide-resolved and residue-resolved FPOP and GEE labeling yields for ApoE3 and ApoE3MM. Panel A plots the residue-resolved significant differences in FPOP yields between the proteins. Each yield difference is normalized to the maximum yield per residue for all residues of the same amino acid type, averaged from all FPOP experiments. Background modification yields observed in the control experiments are subtracted from their corresponding FPOP yields before the relative value is determined. Error bars are determined as described in Figure 1. Significance was determined at 95% confidence by the Student's *t* test. Panel B plots the residue-resolved significant differences in 3 min GEE yields between the proteins. Each yield difference is normalized to the average yield per residue for all acidic residues, averaged from all 3 min GEE experiments. Error bars are the normalized standard errors for the 3 min measurement. Significant difference was defined as at least two GEE labeling time points exhibiting a difference at 95% confidence by the Student's *t* test and having the same sign. The bottom panel shows the residues along the ApoE3 primary sequence exhibiting more labeling in the monomeric mutant. Black-underlined residues convey the significant FPOP labeling difference; red-underlined residues the significant GEE labeling difference.

and ApoE4 have less-reactive Arg at this site. The modification extent of Met also distinguishes ApoE 62-72 from the corresponding peptides of ApoE4 and ApoE3; in this case, ApoE4 is appreciably less labeled than that in ApoE3. A pairwise residue comparison does not resolve this difference at 95% confidence (M64 $p = 0.11$), but the modification levels of M64, E66, and M68 together give rise to peptide signals that are significantly different. This underscores the need to examine footprinting data at several levels of sequence context. The variance in Met and Cys modification yields, although large, is not unusual, owing to the high sensitivity of sulfur-containing residues to endogenous reactive oxygen species and to oxidation during handling before and after the labeling experiment.[17,31,32] The background oxidation values for Met varied from 0.3% for M218 to 36% for M272, consistent with the MS of the unlabeled protein (data not shown).

ApoE3 vs ApoE3MM. It is clear that in the C-terminal and linker domains, the FPOP yields at the residue level of ApoE3MM are higher than those of WT-ApoE3 (Figure 3A and Supporting Information Table 3). This conclusion is based on analysis of 304 unmodified and modified tryptic peptides of ApoE3 and ApoE3MM, from 1182 EIC features comprising 67.2% of all detected features (Supporting Information Table 4). The criteria for inclusion are identical to those applied to the WT isoform experiment. One in four residues is detected as modified. The order of reactivity is nearly identical to that observed for $^{\bullet}$OH footprinting of the WT protein. Figure 3A plots only the residues which are significantly different between ApoE3 and ApoE3MM, at 95% confidence. A total of 26 residues spanning residues 167 to 299 show significantly greater labeling for ApoE3MM, indicating these sites are more solvent-protected in the WT protein than the MM (Figure 3, bottom panel). Clearly, the C-terminal domain is involved in WT oligomerization, as was inferred from previous studies using truncated forms of ApoE proteins.[10,33] The high density of protected sites in regions 183-205 and 232-251 may indicate localized regions of oligomeric interaction in the WT. Other sites in the C-terminal domain cannot fairly be compared. Sites 257, 264, and 287 were detected as modified in both proteins. These are three of the four mutation sites (F257A, W264R, L279Q, and V287E) that together engender monomericity.[34] We do not compare their signals because each residue's inherent $^{\bullet}$OH reactivity is different from its analogue, no matter their possible difference in SASA.

Glycyl Ethyl Ether (GEE) Footprinting. To corroborate the findings in the FPOP monomer/oligomer experiment, we employed a second footprinting approach whereby carboxyl side chains were submitted to GEE modification. As with the FPOP data, quantitation was based on unmodified and modified LC-MS EIC features, with annotation accepted if the precursor ion is within 5 ppm mass tolerance of theory and the product-ion (MS^2) spectra are acceptable. A control whereby

dx.doi.org/10.1021/bi200911c | *Biochemistry* 2011, 50, 8117–8126

the protein is not submitted to modification is unnecessary for this kind of labeling because exogenous background modifications at +85.0528 D are highly unlikely in the protein prior to modification and do not occur during peptide work-up. In the absence of GEE-induced unfolding, the time dependence for the modification level should be monotonic; consequently, we used four GEE exposure times to differentiate more reliably the labeling yields of the acidic residues (Supporting Information Table 5). Two example kinetic plots show that E212 is consistently more modified in ApoE3MM (Figure 4A),

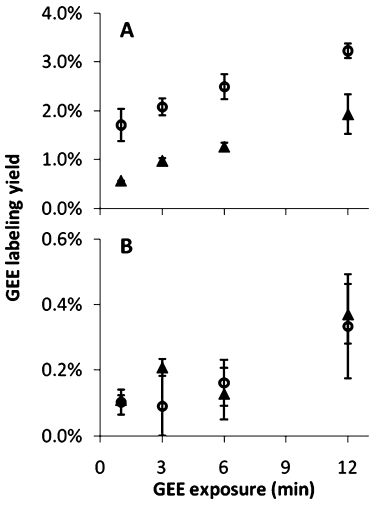

Figure 4. Representative plots of GEE labeling for two residues. Open circles denote ApoE3MM GEE-modified yields at four time points; solid triangles denote the ApoE3 yields. Residue E212 data are shown in plot A. Residue E109 data are shown in plot B.

whereas E109 is labeled nearly identically and at a lower level for both proteins (Figure 4B). This analysis informs a conservative criterion for assigning difference per acidic residue: at 3 min the pairwise Student's *t* test should show a significant difference at 95% confidence, and this trend should also pertain at 6 and 12 min. By this criterion the significantly different residues are plotted in Figure 3B, showing their 3 min labeling yields.

The results from GEE labeling corroborate the findings of the per-residue FPOP results. The bottom pane of Figure 3 shows those residues that are more significantly labeled by FPOP (black) or GEE (red) in the monomeric mutant. The number of significant differences in labeling between ApoE3 and ApoE3MM is substantially greater than those between ApoE3 and ApoE2 and E4, and furthermore, the magnitude of the differences is also greater. By virtue of the normalization discussed above, the magnitude of change measured in the monomer/oligomer experiment is indicative of a larger SASA change between monomer and oligomer than is seen between WT isoforms explored in the first experiment.

DISCUSSION

The importance of ApoE in biomedicine and the difficulty in obtaining high-resolution structural information about this protein family motivated this footprinting study. In vivo, ApoE interacts with multiple partners including low-density lipoprotein receptors (LDLRs), cell-surface heparin sulfate proteoglycans (HSPGs), ATP binding cassette protein 1 (ABCA1), and low-density lipoprotein-related proteins (LRPs).[6,35−38] ApoE binds to lipids and cholesterol with high affinity to form lipoprotein particles.[39,40] Interactions of ApoE with lipids, cholesterol, and the ApoE receptors are crucial ApoE functions.[41,42] ApoE isoforms are also likely to interact with amyloid beta (Aβ) peptides. Interactions with Aβ peptide(s) may contribute to the progression of Alzheimer's disease (AD) in an ApoE isoform-specific manner.[43−46] In vitro, ApoE molecules self-associate to form dimers, tetramers, and even higher aggregates in a concentration, pH, and temperature-dependent manner.[8,47−49] Although formation of dimers and tetramers occurs readily at nanomolar concentrations at physiological pH and room temperature, formation of larger aggregates occurs slowly and requires acidic pH or higher temperature (37 °C) or higher concentrations.[8,48,49] The self-association of ApoE affects binding to lipids and to Aβ.[40,50] Moreover, ApoE aggregates are toxic to neuronal cells.[48] Although the self-association status of ApoE in vivo is not known, ApoE synthesized by macrophages and human embryonic kidney (HEK) cells are poorly lipid associated, apparently because ApoE is self-associated possibly in the tetrameric form.[42,51] Thus, a mechanistic understanding of self-association properties of ApoE can further our understanding of the physiological functions of ApoE and the role of ApoE isoforms in AD. Using mass- spectrometry-based footprinting, we have, for the first time, identified the regions and the residues in the ApoE sequence involved in self-association.

FPOP Yield and SASA. One of FPOP's virtues is that, though the reaction window is short, protein modification occurs with high yield. Consequently, many solvent-exposed residues of marginal reactivity can still be assayed as compared to the same kind of residues in synchrotron radiolysis $^{\bullet}$OH footprinting.[52−54] The average residue labeling yield per amino acid type is similar but not identical to the known reaction rates of $^{\bullet}$OH with free amino acids[55] and to the MS analysis of $^{\bullet}$OH amino amide reaction products.[18] We observe their reactivity order to be Cys > Met > Trp > His > Gln > Tyr > Phe > Asp > Pro > Glu > Leu > Val > Arg > Lys. Differences between inherent and observed reactivity are due to the structural context of residues, as their inherent amino acid reactivity with $^{\bullet}$OH is mitigated by solvent accessibility in a properly controlled footprinting experiment. For example, Gln is less reactive with $^{\bullet}$OH than is Tyr or Phe as a free amino acid or amide. Being more hydrophilic than these residues, however, Gln is likely to be more solvent-exposed in a protein and so may experience a higher level of modification than a more reactive amino acid that is more protected (Supporting Information Table 1, Q21 yield > Y162 yield). Same-day labeling, same-column separation in LC/MS, and the Rosetta Elucidator peak alignment software ensured that the same modified and unmodified-peptide features were used in determining the residue yields for all WT samples. We, therefore, attribute any significant differences in residue yields to differences in solvent-accessible surface areas (SASA) of the isoforms, as all other sources of bias are shared identically.

We would argue that ±15% SASA relative to the maximum SASA for the same kind of residues is a small change. In absolute square angstroms, a 15% change could be less than 5 Å^2 or more than 30 Å^2, depending on the type of residue. Relative to fully exposed side chain surface areas, this is a small area. For example, W20 in the truncated protein ApoE3 1-183 has a SASA value of 199 Å^2, determined by the GETAREA algorithm[56] for the 1kc3.pdb NMR structure.[7] The relative SASA change is due to at least two different protein oligomer conformations. In the simplest scenario, one conformation

would exclusively describe 4 μM ApoE3, and the other would exclusively belong to the other ApoE isoform at 4 μM. In this case, a statistically significant amino acid-relative labeling change is directly attributed to a change in the surface areas of each conformation. If the change were less than 15%, we would conclude the isoform is only slightly more exposed or protected than ApoE3. This is the case for three of the five residues in ApoE4 that are significantly different from their ApoE3 analogues: Y162 and P183 are slightly more exposed, with same amino acid relative changes of 7% and 5%, respectively, whereas E266 is slightly protected, with a relative change of −10% (Figure 1A). Two of the three significantly different residues in ApoE2 compared to ApoE3 are not substantially so: relative to the average of all glutamic acid yields, E255 shows a −17% and E266 a −10% change in labeling (Figure 2A).

Structures of the ApoE Isoforms. The overall structures (mixtures of structures) are nearly the same, within the constraints of footprinting, for the three ApoE isoforms. We arrived at this conclusion by invoking a syllogism: (1) FPOP snapshot labels an ensemble of conformations and complexes at equilibrium.[19,21] (2) Of the 56 residues detected as modified among the isoforms, 95% were modified at statistically equivalent levels for ApoE2 and ApoE3 and 91% were so modified for ApoE3 and ApoE4. (3) Therefore, the overall structures of the ApoE isoforms as measured by this technique are similar with one exception, to be discussed later.

The ApoE proteins were prepared as described by Garai and Frieden[8] in their study of the association−dissociation behavior of ApoE. They determined the isoform monomer, dimer, and tetramer concentrations as a function of the total concentration on the basis of self-association rate constants for a monomer−dimer−tetramer model determined from FRET kinetics measurements and sedimentation velocity experiments. At 4 μM total protein, their model shows that 84% of proteins are tetrameric, irrespective of the ApoE isoform. This is in qualitative agreement with previous sedimentation velocity studies of ApoE in the absence of lipid;[28,29] that study spanned the 4 μM concentration. A reasonable conclusion from the similarity in FPOP response among the ApoE isoforms, given the high prevalence of the tetrameric component in the oligomer state studied here, is that the ApoE2, ApoE3, and ApoE4 tetrameric structures are highly similar.

Despite the strong similarities in overall structure, the region of ApoE4 including M108 is different from that of ApoE2 and E3. Consistent with the high-resolution structures of the N-terminal ApoE3 domain,[6,57] the near lack of M108 modification in ApoE3 and E2 indicates that it is buried, whereas the labeling yield at M108 in ApoE4 shows that it is at least partially solvent-accessible. The exposure of M108 in E4 can occur by an intra- or intermolecular interaction pulling on the 50-79 α-helix (Figure 5). Supporting this model are the M64 and M68 FPOP yields, which are slightly diminished for ApoE4 relative to those for ApoE3. Caution is indicated because the features used to compare both samples to determine the M108 yields are not the same: the C112R mutation differentiating ApoE4 from ApoE3 resides in the same tryptic peptide as M108. This departs from the usual state-to-state comparisons and opens the possibility that causes, in addition to a SASA difference, may give rise to variations in yield. This may also apply to Y162 in the comparison of ApoE2 with ApoE3. Only Y162 is found to be significantly more labeled in ApoE2 than in ApoE3, and it resides in the tryptic R158C peptide.

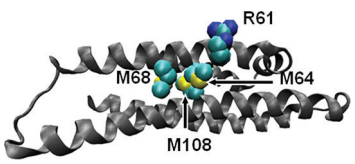

Figure 5. ApoE4 24-162 X-ray crystal structure[63] with R61, M64, M68, and M108 side chains depicted by element type and van der Waals radius.

Solvent Accessibility of N- vs C-terminal Regions. A comparison of the FPOP modification extents for the Trp residues shows that the C-terminal Trp residues are more solvent exposed than the N-terminal Trp residues for each isoform (Supporting Information Table 1). For example, W264 is the most efficiently modified Trp, followed by W276, W210, and then the N-terminus Trp residues. W39 cannot be detected as modified, although the reporting tryptic peptide 39-61 is of low abundance. A similar conclusion was reached by Garai et al.[25] using apoE labeled with ^{19}F tryptophan. Our conclusion arises from a comparison of the FPOP yields for same amino acid residue located throughout the same protein. These intramolecular comparisons may allow more insightful conclusions about protein structure than yield comparisons of same residue in two different protein isoforms. Essentially, residues of the same type may be ranked in order of their yield; those at the top of the list should have the highest SASA.

Regions of Oligomeric Interaction. This is the first experimental study of full-length ApoE that shows that the C-terminal domain is the primary region of self-association in the tetrameric form, as has long been hypothesized.[5,10,11] Westerlund and Weisgraber[10] showed in sedimentation experiments of C-terminal-truncated ApoE3 isoforms that region 267-299 is essential to association. This conclusion was reinforced by using several biophysical techniques for similar truncated ApoE isoforms.[9,28] Furthermore, the 10 kDa C-terminal domain itself oligomerizes.[11] The choice of ApoE3MM used in our study was determined by the observation that substitutions at L179, F257, W264, V269, and V287 resulted in a monomeric form of both the C-terminal domain alone[33] and the full-length ApoE3 protein.[34] A substantial number of residues in the C-terminal and hinge domains are more solvent-accessible in the monomeric mutant than in the ApoE3 WT isoform, whereas modifications of their N-terminal domains are statistically identical. Moreover, this result is demonstrated by two independent footprinting methods, FPOP and GEE labeling (Figure 6), with a high degree of consistency. The FPOP data indicate that although these substitutions demonstrably prevent oligomerization, the region of self-association is larger than that covered by the substitutions, involving the hinge region (ApoE 192-215) as well. That the formation of oligomers requires more than two "patches" for self-association is consistent with our results identifying multiple regions of oligomerization.

In a very recent study, Garai et al.[58] showed that at pH 4.5 the association−dissociation of ApoE is significantly faster than at neutral pH. ApoE-lipid binding is also much stronger at low pH, and this supports the hypothesis that it is the ApoE monomer that primarily binds lipid tightly. In light of this, our finding suggests that a large portion of the protein's C-terminus domain and hinge region must reorganize by oligomeric dissociation before lipid interaction.

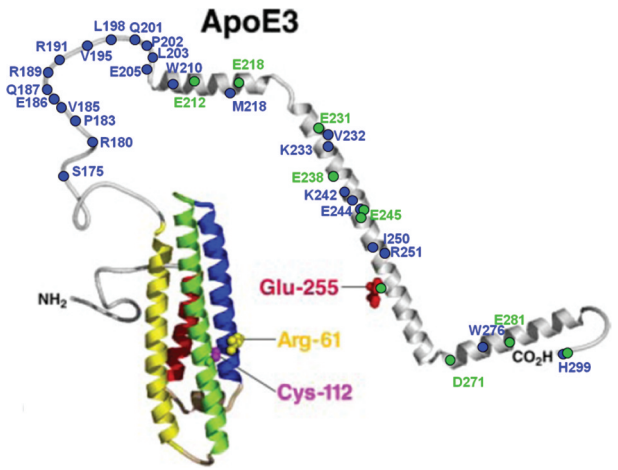

Figure 6. A model of ApoE3[64] shown with marked residues that exhibited a statistically significant increase in labeling in the monomeric mutant. Blue residues were indicated by FPOP labeling and green residues by GEE labeling.

Comparison of GEE and FPOP Footprinting. There is good qualitative agreement between the results from FPOP and those from GEE footprinting; an exception is in the region 183−205 (Figure 3, bottom panel). Although several residues in this region undergo increased FPOP oxidative modification for ApoE3MM, the levels of labeling by GEE at the only two modifiable sites residing in this region (E186 and E205) are the same (Supporting Information Table 5). There are several aspects of GEE and FPOP footprinting germane to ascribing differences in their outcomes. First, the time scale of labeling is dramatically different: the much longer exposure to GEE labeling will sample an conformation averaged over minutes, whereas FPOP may see an ensemble of conformations that fluctuate on a microseconds time scale. Second, the sampling of acidic residues by "priming" with EDC and subsequent reaction with GEE requires an interaction volume that is larger than that of the water molecule, whereas •OH is a probe much the same size as water. Additionally, the sites of reaction on acidic residues are different. Whereas the Glu or Asp carboxylate nucleophile attacks the carbodiimide carbon as a first step,[59] •OH preferentially abstracts hydrogen from the Glu β and γ carbons.[17,60] Thus, the relevant solvent accessibilities for FPOP vs GEE labeling are different for the same residue.

Comparison of the N-Terminal Domains of ApoE2, ApoE3, ApoE4, and ApoE3MM. We find little difference between the labeling footprints of the N-terminal domains for the WT isoforms and between ApoE3 and its monomeric mutant isoform (Figures 1, 2, and 3). Thus, the WT isoforms must adopt similar N-terminal structures as that of the monomeric mutant. In an unpublished study examining the ApoE3MM data, we propose that it adopts an N-terminal domain structure much like the most recent NMR ApoE3 1-183 structure.[7] With few exceptions, the rank order of yields of ApoE3 residues detected as modified in the first and second experiment are the same, although the levels of modification are higher in the ApoE3 monomer/oligomer study owing to the doubling of H_2O_2 starting material. Some of the detected oxidative modifications in the latter case may be due to secondary protein−peroxy reactions that do not sample the equilibrium structure,[61] but such a signal cannot account for the overwhelming differences seen between ApoE3 and ApoE3MM.

CONCLUSIONS

At 4 μM, WT-ApoE2, ApoE3, and ApoE4 must exit in solution as similar structures. At micromolar concentrations the proteins are primarily tetramers, as shown in other work.[8] Our data are also consistent with the assignment of a four-helix bundle structure in the N-terminal domain of the 299 amino acid monomeric mutant of ApoE3. Although the overall structures of the isoforms are similar, that of region M108 in E4 is significantly different. This may be due to a real change in SASA, or to a difference in the ionization response of the peptides that carry the isoform mutation C112R, or both. By virtue of the per-residue trends drawn from two independent MS-based footprinting data sets of ApoE3 and ApoE3MM, we conclude that residues in the hinge and C-terminus domains, especially spanning 183-205 and 232-251, are involved in inter- and intramolecular interactions concomitant with self-association of ApoE3. Owing to their sequence invariance in this region, we suggest that the same oligomerization interaction also occurs for ApoE2 and ApoE4.

The oligomer regions of interaction are derived from two independent covalent footprinting approaches that show remarkable concordance in mapping the C-terminal domain interaction. The sensitivity and nonselectivity advantages of hydroxyl radical footprinting are highlighted by the discovery that the dynamic hinge region is also involved in oligomerization; this region is sparsely populated by the GEE labeling substrate and so is silent to such a method.

One advantage of MS-based protein footprinting is that it can sample physiologic mixtures. Thus, we plan future studies to characterize ApoE in the presence of Aβ peptides both with and without the context of lipoproteins. This should be possible at high sequence resolution and may reveal interactions implied in the genetic association of ApoE4 with Alzheimer's disease.[62]

ASSOCIATED CONTENT

Supporting Information

Five tables that compare the per-residue labeling yields and observed peptides of the WT isoforms and of ApoE3 and its MM. This material is available free of charge via the Internet at http://pubs.acs.org.

AUTHOR INFORMATION

Corresponding Author

*Phone: (314) 935-4814. Fax: (314) 935-7484. E-mail: mgross@wustl.edu.

ACKNOWLEDGMENTS

This work was supported by the NIH National Center for Research Resources (P41 RR000954).

ABBREVIATIONS

FPOP, fast photochemical oxidation of proteins; GEE, glycine ethyl ester; ApoE2, apolipoprotein E isoform E2; ApoE3, apolipoprotein E isoform E3; ApoE4, apolipoprotein E isoform E4; ApoE3MM, monomeric mutant of apolipoprotein E isoforms E3; TCEP, tris(2-carboxyethyl)phosphine hydrochloride; WT, wild type; SASA, solvent accessible surface area; PBS, phosphate buffered saline; βME, β-mercaptoethanol;

DTT, dithiolthreitol; EDC, 1-ethyl-3-(3-(dimethylamino)-propyl)carbodiimide; ESI, electrospray ionization; MS, mass spectrometry; LC, liquid chromatography.

REFERENCES

(1) Mahley, R. W. (1988) Apolipoprotein E: cholesterol transport protein with expanding role in cell biology. *Science 240*, 622−630.

(2) Strittmatter, W. J., Saunders, A. M., Schmechel, D., Pericak-Vance, M., Enghild, J., Salvesen, G. S., and Roses, A. D. (1993) Apolipoprotein E: high-avidity binding to beta-amyloid and increased frequency of type 4 allele in late-onset familial Alzheimer disease. *Proc. Natl. Acad. Sci. U. S. A. 90*, 1977−1981.

(3) Corder, E. H., Saunders, A. M., Strittmatter, W. J., Schmechel, D. E., Gaskell, P. C., Small, G. W., Roses, A. D., Haines, J. L., and Pericak-Vance, M. A. (1993) Gene dose of apolipoprotein E type 4 allele and the risk of Alzheimer's disease in late onset families. *Science 261*, 921−923.

(4) Bu, G. (2009) Apolipoprotein E and its receptors in Alzheimer's disease: pathways, pathogenesis and therapy. *Nat. Rev. Neurosci. 10*, 333−344.

(5) Weisgraber, K. H. (1994) Apolipoprotein E: Structure-Function Relationships. *Adv. Protein Chem. 45*, 249−302.

(6) Wilson, C., Wardell, M. R., Weisgraber, K. H., Mahley, R. W., and Agard, D. A. (1991) Three-dimensional structure of the LDL receptor-binding domain of human apolipoprotein E. *Science 252*, 1817−1822.

(7) Sivashanmugam, A., and Wang, J. (2009) A Unified Scheme for Initiation and Conformational Adaptation of Human Apolipoprotein E N-terminal Domain upon Lipoprotein Binding and for Receptor Binding Activity. *J. Biol. Chem. 284*, 14657−14666.

(8) Garai, K., and Frieden, C. (2010) The Association-Dissociation Behavior of the ApoE Proteins: Kinetic and Equilibrium Studies. *Biochemistry 49*, 9533−9541.

(9) Sakamoto, T., Tanaka, M., Vedhachalam, C., Nickel, M., Nguyen, D., Dhanasekaran, P., Phillips, M. C., Lund-Katz, S., and Saito, H. (2008) Contributions of the Carboxyl-Terminal Helical Segment to the Self-Association and Lipoprotein Preferences of Human Apolipoprotein E3 and E4 Isoforms. *Biochemistry 47*, 2968−2977.

(10) Westerlund, J. A., and Weisgraber, K. H. (1993) Discrete carboxyl-terminal segments of apolipoprotein E mediate lipoprotein association and protein oligomerization. *J. Biol. Chem. 268*, 15745−15750.

(11) Aggerbeck, L. P., Wetterau, J. R., Weisgraber, K. H., Wu, C. S., and Lindgren, F. T. (1988) Human apolipoprotein E3 in aqueous solution. II. Properties of the amino- and carboxyl-terminal domains. *J. Biol. Chem. 263*, 6249−6258.

(12) Yokoyama, S., Kawai, Y., Tajima, S., and Yamamoto, A. (1985) Behavior of human apolipoprotein E in aqueous solutions and at interfaces. *J. Biol. Chem. 260*, 16375−16382.

(13) Chen, J., Li, Q., and Wang, J. (2011) Topology of human apolipoprotein E3 uniquely regulates its diverse biological functions. *Proc. Natl. Acad. Sci. U.S.A.*

(14) Hambly, D. M., and Gross, M. L. (2006) In *The Encyclopedia of Mass Spectrometry: Ionization Methods* (Gross, M. L., and Caprioli, R. M., Eds.).

(15) Guan, J.-Q., and Chance, M. R. (2005) Structural proteomics of macromolecular assemblies using oxidative footprinting and mass spectrometry. *Trends Biochem. Sci. 10*, 583−592.

(16) Aebersold, R., and Mann, M. (2003) Mass spectrometry-based proteomics. *Nature 422*, 198−207.

(17) Xu, G., and Chance, M. R. (2007) Hydroxyl Radical-Mediated Modification of Proteins as Probes for Structural Proteomics. *Chem. Rev. 107*, 3514−3543.

(18) Xu, G., and Chance, M. R. (2005) Radiolytic Modification and Reactivity of Amino Acid Residues Serving as Structural Probes for Protein Footprinting. *Anal. Chem. 77*, 4549−4555.

(19) Hambly, D. M., and Gross, M. L. (2005) Laser Flash Photolysis of Hydrogen Peroxide to Oxidize Protein Solvent-Accessible Residues on the Microsecond Timescale. *J. Am. Soc. Mass Spectrom. 16*, 2057−2063.

(20) Aye, T. T., Low, T. Y., and Sze, S. K. (2005) Nanosecond Laser-Induced Photochemical Oxidation Method for Protein Surface Mapping with Mass Spectrometry. *Anal. Chem. 77*, 5814−5822.

(21) Gau, B. C., Sharp, J. S., Rempel, D. L., and Gross, M. L. (2009) Fast Photochemical Oxidation of Protein Footprints Faster than Protein Unfolding. *Anal. Chem. 81*, 6563−6571.

(22) Wen, J., Zhang, H., Gross, M. L., and Blankenship, R. E. (2009) Membrane orientation of the FMO antenna protein from Chlorobaculum tepidum as determined by mass spectrometry-based footprinting. *Proc. Natl. Acad. Sci. U. S. A. 106*, 6134−6139.

(23) Swaisgood, H., and Natake, M. (1973) Effect of Carboxyl Group Modification on Some of the Enzymatic Properties of L-Glutamate Dehydrogenase. *J. Biochem. 74*, 77−86.

(24) Hoare, D. G., and Koshland, D. E. (1967) A Method for the Quantitative Modification and Estimation of Carboxylic Acid Groups in Proteins. *J. Biol. Chem. 242*, 2447−2453.

(25) Garai, K., Mustafi, S. M., Baban, B., and Frieden, C. (2009) Structural differences between apolipoprotein E3 and E4 as measured by 19F NMR. *Protein Sci. 19*, 66−74.

(26) Xu, G., Kiselar, J., He, Q., and Chance, M. R. (2005) Secondary Reactions and Strategies To Improve Quantitative Protein Footprinting. *Anal. Chem. 77*, 3029−3037.

(27) Vidavsky, I., Rempel, D. L., Gross, M. L. (2006) 2D Mass Spectra Correlation − Semi Automatic Tool for Modified Peptide Discovery, in *Proceedings of the 54th ASMS Conference on Mass Spectrometry and Allied Topics*, Seattle, WA.

(28) Chou, C.-Y., Lin, Y.-L., Huang, Y.-C., Sheu, S.-Y., Lin, T.-H., Tsay, H.-J., Chang, G.-G., and Shiao, M.-S. (2005) Structural Variation in Human Apolipoprotein E3 and E4: Secondary Structure, Tertiary Structure, and Size Distribution. *Biophys. J. 88*, 455−466.

(29) Perugini, M. A., Schuck, P., and Howlett, G. J. (2000) Self-association of Human Apolipoprotein E3 and E4 in the Presence and Absence of Phospholipid. *J. Biol. Chem. 275*, 36758−36765.

(30) Xu, G., and Chance, M. R. (2005) Radiolytic Modification of Sulfur-Containing Amino Acid Residues in Model Peptides: Fundamental Studies for Protein Footprinting. *Anal. Chem. 77*, 2437−2449.

(31) Hawkins, C. L., Morgan, P. E., and Davies, M. J. (2009) Quantification of protein modification by oxidants. *Free Radical Biol. Med. 46*, 965−988.

(32) Morand, K., Talbo, G., and Mann, M. (1993) Oxidation of peptides during electrospray ionization. *Rapid Commun. Mass Spectrom. 7*, 738−743.

(33) Fan, D., Li, Q., Korando, L., Jerome, W. G., and Wang, J. (2004) A monomeric human apolipoprotein E carboxyl-terminal domain. *Biochemistry 43*, 5055−5064.

(34) Zhang, Y., Vasudevan, S., Sojitrawala, R., Zhao, W., Cui, C., Xu, C., Fan, D., Newhouse, Y., Balestra, R., Jerome, W. G., Weisgraber, K., Li, Q., and Wang, J. (2007) A Monomeric, Biologically Active, Full-Length Human Apolipoprotein E. *Biochemistry 46*, 10722−10732.

(35) Narita, M., Holtzman, D. M., Fagan, A. M., LaDu, M. J., Yu, L., Han, X., Gross, R. W., Bu, G., and Schwartz, A. L. (2002) Cellular Catabolism of Lipid Poor Apolipoprotein E via Cell Surface LDL Receptor-Related Protein. *J. Biochem. 132*, 743−749.

(36) Ruiz, J., Kouiavskaia, D., Migliorini, M., Robinson, S., Saenko, E. L., Gorlatova, N., Li, D., Lawrence, D., Hyman, B. T., Weisgraber, K. H., and Strickland, D. K. (2005) The apoE isoform binding properties of the VLDL receptor reveal marked differences from LRP and the LDL receptor. *J. Lipid Res. 46*, 1721−1731.

(37) Weisgraber, K. H., Rall, S. C., Mahley, R. W., Milne, R. W., Marcel, Y. L., and Sparrow, J. T. (1986) Human apolipoprotein E. Determination of the heparin binding sites of apolipoprotein E3. *J. Biol. Chem. 261*, 2068−2076.

(38) Krimbou, L., Denis, M., Haidar, B., Carrier, M., Marcil, M., and Genest, J. (2004) Molecular interactions between apoE and ABCA1. *J. Lipid Res. 45*, 839−848.

(39) Lund-Katz, S., and Phillips, M. C. (2010) High density lipoprotein structure-function and role in reverse cholesterol transport. *Subcell Biochem. 51*, 183−227.
(40) Garai, K., Baban, B., and Frieden, C. (2011) Dissociation of apoE oligomers to monomers is required for high affinity binding to phospholipid vesicles. *Biochemistry 50*, 2550−2558.
(41) Lin, C.-Y., Duan, H., and Mazzone, T. (1999) Apolipoprotein E-dependent cholesterol efflux from macrophages: kinetic study and divergent mechanisms for endogenous versus exogenous apolipoprotein E. *J. Lipid Res. 40*, 1618−1626.
(42) Langer, C., Huang, Y., Cullen, P., Wiesenhutter, B., Mahley, R. W., Assmann, G., and von Eckardstein, A. (2000) Endogenous apolipoprotein E modulates cholesterol efflux and cholesteryl ester hydrolysis mediated by high-density lipoprotein-3 and lipid-free apolipoproteins in mouse peritoneal macrophages. *J. Mol. Med. 78*, 217−227.
(43) Strittmatter, W. J., Saunders, A. M., Schmechel, D., Pericak-Vance, M., Enghild, J., Salvesen, G. S., and Roses, A. D. (1993) Apolipoprotein E: high-avidity binding to beta-amyloid and increased frequency of type 4 allele in late-onset familial Alzheimer disease. *Proc. Natl. Acad. Sci. U. S. A. 90*, 1977−1981.
(44) Naslund, J., Thyberg, J., Tjernberg, L. O., Wernstedt, C., Karlstrom, A. R., Bogdanovic, N., Gandy, S. E., Lannfelt, L., Terenius, L., and Nordstedt, C. (1995) Characterization of stable complexes involving apolipoprotein E and the amyloid beta peptide in Alzheimer's disease brain. *Neuron 15*, 219−228.
(45) Manelli, A.M., Bulfinch, L. C., Sullivan, P. M., and LaDu, M. J. (2007) Abeta42 neurotoxicity in primary co-cultures: Effect of apoE isoform and Abeta conformation. *Neurobiol. Aging 28*, 1139−1147.
(46) Holtzman, D. M., Bales, K. R., Tenkova, T., Fagan, A. M., Parsadanian, M., Sartorius, L. J., Mackey, B., Olney, J., McKeel, D., Wozniak, D., and Paul, S. M. (2000) Apolipoprotein E isoform-dependent amyloid deposition and neuritic degeneration in a mouse model of Alzheimer's disease. *Proc. Natl. Acad. Sci. U. S. A. 97*, 2892−2897.
(47) Aggerbeck, L. P., Wetterau, J. R., Weisgraber, K. H., Wu, C. S., and Lindgren, F. T. (1988) Human apolipoprotein E3 in aqueous solution. II. Properties of the amino- and carboxyl-terminal domains. *J. Biol. Chem. 263*, 6249−6258.
(48) Hatters, D. M., Zhong, N., Rutenber, E., and Weisgraber, K. H. (2006) Amino-terminal domain stability mediates apolipoprotein E aggregation into neurotoxic fibrils. *J. Mol. Biol. 361*, 932−944.
(49) Garai, K., Baban, B., and Frieden, C. (2011) Self-Association and Stability of the ApoE Isoforms at Low pH: Implications for ApoE-Lipid Interactions. *Biochemistry 50*, 6356−6364.
(50) Chan, W., Fornwald, J., Brawner, M., and Wetzel, R. (1996) Native complex formation between apolipoprotein E isoforms and the Alzheimer's disease peptide A beta. *Biochemistry 35*, 7123−7130.
(51) LaDu, M. J., Stine, W. B., Narita, M., Getz, G. S., Reardon, C. A., and Bu, G. (2005) Self-Assembly of HEK Cell-Secreted ApoE Particles Resembles ApoE Enrichment of Lipoproteins as a Ligand for the LDL Receptor-Related Proteinâ€. *Biochemistry 45*, 381−390.
(52) Guan, J. Q., Vorobiev, S., Almo, S. C., and Chance, M. R. (2002) Mapping the G-Actin Binding Surface of Cofilin Using Synchrotron Protein Footprinting. *Biochemistry 41*, 5765−5775.
(53) Maleknia, S. D., Ralston, C. Y., Brenowitz, M. D., Downard, K. M., and Chance, M. R. (2001) Determination of Macromolecular Folding and Structure by Synchrotron X-Ray Radiolysis Techniques. *Anal. Biochem. 289*, 103−115.
(54) Goldsmith, S. C., Guan, J.-Q., Almo, S. C., and Chance, M. R. (2001) Synchrotron Protein Footprinting: A Technique to Investigate Protein-Protein Interactions. *J. Biomol. Struct. Dyn. 19*, 405−419.
(55) Buxton, G. V., Greenstock, C. L., Helman, W. P., and Ross, A. B. (1988) Critical Review of Rate Constants for Reactions of Hydrated Electrons, Hydrogen Atoms and Hydroxyl Radicals (*OH/*O-) in Aqueous Solution. *J. Phys. Chem. Ref. Data 17*, 513−886.
(56) Gerstein, M. (1992) A resolution-sensitive procedure for comparing protein surfaces and its application to the comparison of antigen-combining sites. *Acta Crystallogr., Sect. A 48*, 271−276.
(57) Sivashanmugam, A., and Wang, J. (2009) A complete receptor binding domain of human apolipoprotein E, Wayne State University School of Medicine.
(58) Garai, K., Baban, B., and Frieden, C. (2011) Self-Association and Stability of the ApoE Isoforms at Low pH: Implications for ApoE−Lipid Interactions. *Biochemistry 50*, 6356−6364.
(59) Hermanson, G. T. (2008) *Bioconjugate Techniques*, 2nd ed., Elsevier, Amsterdam.
(60) Garrison, W. M. (1987) Reaction mechanisms in the radiolysis of peptides, polypeptides, and proteins. *Chem. Rev. 87*, 381−398.
(61) Saladino, J., Liu, M., Live, D., and Sharp, J. S. (2009) Aliphatic Peptidyl Hydroperoxides as a Source of Secondary Oxidation in Hydroxyl Radical Protein Footprinting. *J. Am. Soc. Mass Spectrom. 20*, 1123−1126.
(62) Zhong, N., and Weisgraber, K. H. (2009) Understanding the Association of Apolipoprotein E4 with Alzheimer Disease: Clues from Its Structure. *J. Biol. Chem. 284*, 6027−6031.
(63) Dong, L. M., Wilson, C., Wardell, M. R., Simmons, T., Mahley, R. W., Weisgraber, K. H., and Agard, D. A. (1994) Human apolipoprotein E. Role of arginine 61 in mediating the lipoprotein preferences of the E3 and E4 isoforms. *J. Biol. Chem. 269*, 22358−22365.
(64) Hatters, D. M., Peters-Libeu, C. A., and Weisgraber, K. H. (2006) Apolipoprotein E structure: insights into function. *Trends Biochem. Sci. 31*, 445−454.